Molecular-dynamics study of the nematic-isotropic interface

Nobuhiko Akino,[1] Friederike Schmid,[2] and Michael P. Allen[3]

[1]*Max-Planck-Institut für Polymerforschung, Postfach 3148, D-55021 Mainz, Germany*
[2]*Fakultät für Physik, Universität Bielefeld, Universitätsstrasse 25, D-33615 Bielefeld, Germany*
[3]*H. H. Wills Physics Laboratory, University of Bristol, Royal Fort, Tyndall Avenue, Bristol BS8 1TL, United Kingdom*

We present large-scale molecular-dynamics simulations of a nematic-isotropic interface in a system of repulsive ellipsoidal molecules, focusing in particular on the capillary-wave fluctuations of the interfacial position. The interface anchors the nematic phase in a planar way, i.e., the director aligns parallel to the interface. Capillary waves in the direction parallel and perpendicular to the director are considered separately. We find that the spectrum is anisotropic, the amplitudes of capillary waves being larger in the direction perpendicular to the director. In the long-wavelength limit, however, the spectrum becomes isotropic and compares well with the predictions of a simple capillary-wave theory.

I. INTRODUCTION

Surfaces and interfaces in liquid crystals have been the subject of much interest both from a fundamental point of view and because of their practical importance in the context of liquid-crystal devices [1,2]. Liquid crystals are formed by anisotropic particles. Depending on temperature and density, they exhibit various liquid phases. Here, we shall be concerned with the isotropic phase (I), which is an ordinary fully symmetric fluid phase, and the nematic phase (N), where the fluid retains the translational symmetry in all directions (no positional order), but exhibits long-range orientational order. According to a very general symmetry argument, the transition between the isotropic and the nematic phase is first order [1]. Therefore there exist regions in phase space where nematic and isotropic fluids coexist and are separated by interfaces.

The nematic state is characterized by a so-called nematic director, which specifies the preferred direction of alignment of the particles. Surfaces and interfaces break the isotropy of space and usually favor a certain director orientation. This effect, called surface *anchoring*, is commonly characterized by the tilt angle θ between the preferred orientation and the surface (interface) normal, and the anchoring strength or anchoring energy. In particular, the cases $\theta = 0°$ (perpendicular alignment) and $\theta = 90°$ (parallel alignment) are often referred to as homeotropic anchoring and planar anchoring, respectively.

Theoretically, particular attention has been given to N-I interfaces in systems of hard particles. Studies of N-I interfaces in hard-rod systems based on Onsager's approach [3] have indicated that the surface-free energy has a minimum when the rods lie parallel to the interface [4,5], suggesting that the anchoring in this system is planar. Similar results have been obtained in systems of hard ellipsoids [6]. According to the Onsager theory, the interfaces are flat, i.e., fluctuations of the interface position (capillary waves) are not present.

In general, however, one would expect such fluctuations in fluid-fluid interfaces. The usual simple argument reads as follows: On very large length scales, the free energy of a

system containing an interface should be governed by the interfacial tension γ. Let us neglect bubbles and overhangs and parametrize the local position of a fluctuating planar interface by a single-valued function $h(x,y)$. Fluctuations enlarge the interfacial area and thus cost the free energy [7,8]

$$\mathcal{F}_{CW}\{h\} = \frac{\gamma}{2} \int dx\,dy \left[\left(\frac{\partial h}{\partial x} \right)^2 + \left(\frac{\partial h}{\partial y} \right)^2 \right], \qquad (1)$$

(assuming small distortions with $|\partial h/\partial x|, |\partial h/\partial y| \ll 1$). Since this free-energy functional is quadratic, the partition function can be evaluated exactly. $\mathcal{F}\{h\}$ is easily diagonalized by means of a two-dimensional Fourier transform. One finds that the squared amplitude of fluctuations with wave vector $\mathbf{q}$ is on average given by

$$\langle |h(\mathbf{q})|^2 \rangle = \frac{k_B T}{\gamma q^2}, \qquad (2)$$

i.e., *diverges* in the long-wavelength limit $\mathbf{q} \to 0$. The argument thus not only predicts on fairly general grounds the existence of capillary waves at all temperatures, but also that they are actually quite large.

On the other hand, it has been argued that the Onsager approach should be exact in the limit of infinitely elongated particles [9]. The Onsager theory assumes that the structure of the fluid is entirely determined by the second virial coefficient, i.e., by the statistical properties of clusters of two particles. In systems of very long, very thin particles, the probability that one particle interacts with more than one other particle approaches zero, and the Onsager assumption becomes exact. One concludes that capillary waves should vanish in this limit, in contradiction to the argument presented just above.

How can this be? Two explanations are conceivable. First, capillary waves vanish if the interfacial tension diverges. However, this is unlikely here, since the coexistence density of the nematic and the isotropic phase moves towards zero as the particle elongation is increased. Second, capillary waves might be suppressed by long-range interactions, which are disregarded in the functional (1). Indeed, elastic long-range

interactions are present in the nematic phase. We recall that the interface orients the director of the nematic liquid in a certain direction. Long-range interface fluctuations therefore lead to long-range elastic distortions of the director field, which are penalized.

In order to shed more light on these issues, we have carried out extensive molecular-dynamics simulations of an N-I interface in a system of over 100 000 particles of elongation 15:1, and analyzed the capillary-wave spectrum in detail.

To our knowledge, there exist only a few numerical studies of N-I interfaces [10,6,11]. In one of them [10], a system of molecules with a length-to-width ratio $\kappa=3$ interacting via a Gay-Berne potential [12] was studied in a simulation box with a temperature inhomogeneity, which served to make and maintain the N-I interface. The molecules in the nematic phase were found to align parallel to the interface (planar anchoring). However, due to the use of the temperature inhomogeneity, the system is not at thermodynamic equilibrium. Capillary waves of the interface position fluctuations are obviously suppressed. In the other studies [6,11], repulsive ellipsoids of revolution of axis ratio $\kappa=15$ were used in a system confined between two hard walls. The interactions of the walls with molecules were systematically varied to study the interplay between surface and interface anchoring. Planar alignment at the N-I interface was again observed. The system sizes considered were too small to allow for an analysis of capillary waves.

The present work builds on Ref. [11]. We study N-I interfaces in a very large system of repulsive ellipsoids by means of extensive computer simulations, focusing in particular on the capillary-wave fluctuations of the interfaces. The paper is organized as follows: In Sec. II, we describe the model and some simulation details. Section III explains our way to determine the local position of the interface. The results are described and summarized in Sec. IV.

II. MODEL AND SIMULATION DETAILS

Our system consists of an idealized ellipsoidal particles with elongation $\kappa=\sigma_l/\sigma_s=15$ where σ_l and σ_s are the length and width of the particles, respectively. The large value of the elongation $\kappa=15$ ensures that the order of the transition is fairly strong, which makes it easier to generate and maintain the interface. The interaction between two ellipsoids i and j is given by

$$V(\mathbf{u}_i,\mathbf{u}_j,\mathbf{r}_{ij})=\begin{cases}4\epsilon\left(X^{12}-X^6+\dfrac{1}{4}\right),&X^6>\dfrac{1}{2}\\0,&\text{otherwise}\end{cases}\quad(3)$$

with

$$X=\frac{\sigma_s}{r-\sigma(\mathbf{u}_i,\mathbf{u}_j,\hat{\mathbf{r}}_{ij})+\sigma_s}.\quad(4)$$

Here $\mathbf{u}_i$ and $\mathbf{u}_j$ are the orientations of ellipsoids i and j, and $\mathbf{r}_{ij}$ is the center-center vector between the ellipsoids, of mag-

nitude r and direction $\hat{\mathbf{r}}_{ij}$. The distance function σ [13] approximates the contact distance between two ellipsoids and is given by

$$\sigma(\mathbf{u}_i,\mathbf{u}_j,\hat{\mathbf{r}})=\sigma_s\left\{1-\frac{\chi}{2}\left[\frac{(\mathbf{u}_i\cdot\hat{\mathbf{r}}+\mathbf{u}_j\cdot\hat{\mathbf{r}})^2}{1+\chi\mathbf{u}_i\cdot\mathbf{u}_j}\right.\right.$$
$$\left.\left.+\frac{(\mathbf{u}_i\cdot\hat{\mathbf{r}}-\mathbf{u}_j\cdot\hat{\mathbf{r}})^2}{1-\chi\mathbf{u}_i\cdot\mathbf{u}_j}\right]\right\}^{-1/2},\quad(5)$$

where the parameter χ is related to the elongation $\kappa\equiv\sigma_l/\sigma_s$ through

$$\chi=\frac{\kappa^2-1}{\kappa^2+1}.\quad(6)$$

Since the attractive tail of the potential equation (3) has been cut off, its range is much shorter than that of the Gay-Berne potential. This enables us to simulate systems with a large number of particles, which is essential to study the capillary wave effects of interest to us. For convenience, $\sigma_s=1$ defines a unit of length, $\epsilon=1$ a unit of energy, and we take particle mass $m=1$; the particle moment of inertia is set at $I=50m\sigma_s^2$.

As a preliminary run, we performed a molecular-dynamics (MD) simulation of a system with 7200 molecules at constant volume in a box geometry $(L_x:L_y:L_z)=(1:1:8)$ with periodic boundary conditions in all directions. The density was chosen in the coexistence region, $\rho=0.017/\sigma_s^3$, and the temperature $k_BT/\epsilon=1$. A nematic slab bounded by two interfaces parallel to the xy plane assembled as a result. More than 5.5×10^6 MD steps were required to equilibrate this system, where each step covers 0.002 time units. The last configuration was then reproduced four times in the x and y direction, which generated a system with $N=115\,200$ molecules and box size $L_x=L_y=150.1958\sigma_s\equiv L$ and $L_z=300.3916\sigma_s$. This was used as the starting point for a MD simulation of 4.2×10^6 MD steps.

III. BLOCK ANALYSIS AND THE DIVIDING SURFACE

In order to study the interfacial position fluctuations as a function of the system size, one can either perform simulations of various system sizes or simulate a single (large) system and analyze subsystems of it. In this study, we took the latter approach. We split our system of size $L\times L\times L_z$ into columns of block size $B\times B$ and height L_z. The columns are further divided into $N_{\text{bins}}=200$ bins in the z direction. The local position of the interface $z_{\text{int}}(x,y)$ [14] in each column is estimated as follows.

First, we compute the local ordering tensor $\mathbf{S}$ in each bin [of size $B\times B\times(L_z/N_{\text{bins}})$], defined as

$$S_{\alpha\beta}=\frac{1}{n}\sum_{i=1}^{n}\frac{1}{2}(3u_{i\alpha}u_{i\beta}-\delta_{\alpha\beta}),\quad(7)$$

where $u_{i\alpha}$ is the α component of the unit vector which points along the axis of the ith molecule ($\alpha=x,y,z$), and n is the
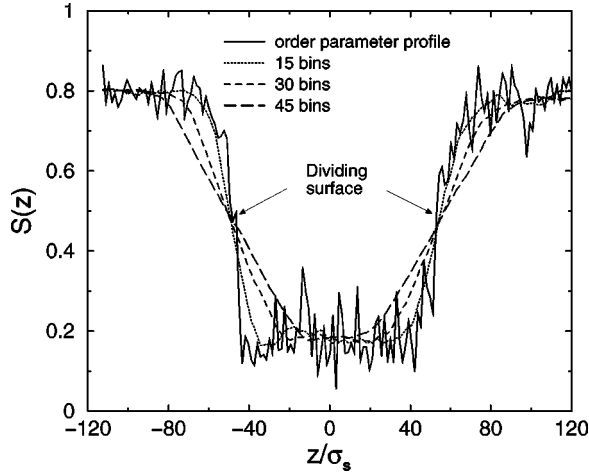
FIG. 1. Illustration of our method of estimating the dividing surface. Solid line shows an example of an order-parameter profile for one of 16 columns with $B = L/4$. Dotted, dashed, and long-dashed lines show averages of this profile over $N_{ave} = 15$, 30, and 45 bins, respectively. We defined the position of the interface z_{int} to be the intersection of the two profiles averaged with $N_{ave} = 15$ and $N_{ave} = 30$.

number of molecules in the bin. The nematic order-parameter $S(z)$ in the bin centered at z is given by the largest eigenvalue of the ordering tensor. The further procedure is illustrated in Fig. 1. Once the order parameter profile $S(z)$ is obtained (solid line), we compute at least two averaged profiles over N_{ave} bins, where N_{ave} is chosen such that an averaged profile still reflects the existence of the interface, but short-range fluctuations are averaged out (dotted and dashed lines in Fig. 1). Finally, the position of the interface is estimated as the intersection of two averaged profiles.

The method is motivated by the following consideration: If the order parameter $S(z)$ did not fluctuate at all in the bulk, the intersection would locate a ''dividing surface,'' where the negative order-parameter excess on the nematic side just balances the positive order-parameter excess on the isotropic side. It should then be independent of N_{ave}, as long as $L\,N_{ave}/N_{bins}$ is larger than the interfacial width and smaller than the total width of the nematic slab. This is not exactly true in an actual configuration due to the bulk fluctuations of $S(z)$, but the method still works well even for small block sizes (see Fig. 2).

IV. RESULTS

The fluctuations of the total director (the direction of the eigenvalue corresponding to the largest eigenvalue of the total ordering tensor) turned out to be so slow that the director hardly changed throughout the run. It always pointed in the y direction. This made it convenient to resolve wave-vector components along and perpendicular to the director, without the need to apply any kind of director constraint.

We used the procedure sketched in Sec. III to determine the local deviations $h(x,y) = z_{int}(x,y) - \bar{z}_{int}$ of the local interface position from its average for various block sizes B. The landscape obtained for the block size $B = L/8$ was further
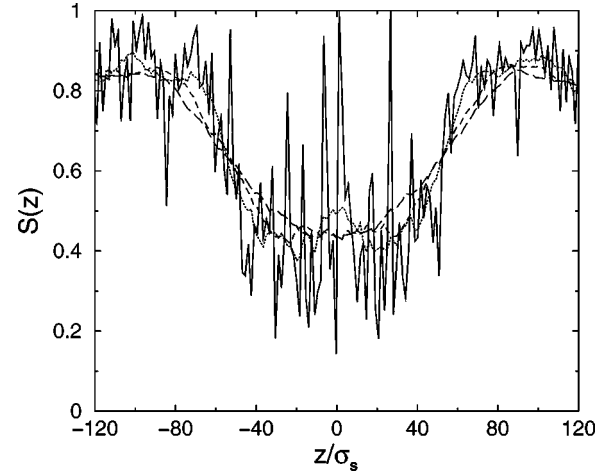

FIG. 2. Same as Fig. 1 but for $B = L/10$. The fluctuations in the order-parameter profile are much larger.

analyzed and Fourier transformed. Fourier modes $h(\mathbf{q})$ are labeled by $\mathbf{n} = (n_x, n_y)$, where n_x and n_y are positive integers with $\mathbf{q} = (2\pi/L)\mathbf{n}$.

First, we inspect the relaxation times and the correlation times of the Fourier modes. The time evolution of the modes $\mathbf{n} = (0,1)$, $(1,0)$, $(0,4)$, and $(4,0)$ is shown as a function of time (in MD steps) in Fig. 3. From there we estimate the number of MD steps needed to equilibrate the system. For the slowest mode $\mathbf{n} = (0,1)$, in the direction parallel to the director, the equilibration process seems to require roughly 1.0×10^6 MD steps. Based on this information, we have discarded the initial 1.2×10^6 MD steps, and collected results over the following 2.96×10^6 MD steps only.

One also has to ensure that the total length of our simulation run significantly exceeds the characteristic time scale of the slowest capillary-wave mode. In order to check this, we have computed the autocorrelation functions of the squared amplitude of the Fourier modes $h(\mathbf{q})$

$$C_{hh}(t) = \frac{\langle |h(t)|^2 |h(0)|^2 \rangle - \langle |h|^2 \rangle^2}{\langle |h|^4 \rangle - \langle |h|^2 \rangle^2} \propto e^{-t/\tau}. \qquad (8)$$

They are shown in Fig. 4 for the slowest Fourier modes in the direction normal to the director $\mathbf{n} = (1,0)$ and parallel to the director $\mathbf{n} = (0,1)$. The correlation time is estimated from the slope of the fitted line as $\tau \approx 1.0 \times 10^5$ MD steps for the $(1,0)$ mode and $\tau \approx 3.0 \times 10^5$ MD steps for the $(0,1)$ mode. This is only by a factor of 10 smaller than the length of the total simulation run. Hence the statistical error of our results is quite large.

We can now proceed to compare our results with the predictions of the capillary-wave theory.

First, we consider the distribution of $h(x,y)$. From the free-energy functional (1), one derives the exact prediction [15]

$$P(h) = \frac{1}{\sqrt{2\pi s^2}} \exp\left(-\frac{h^2}{2s^2}\right), \qquad (9)$$
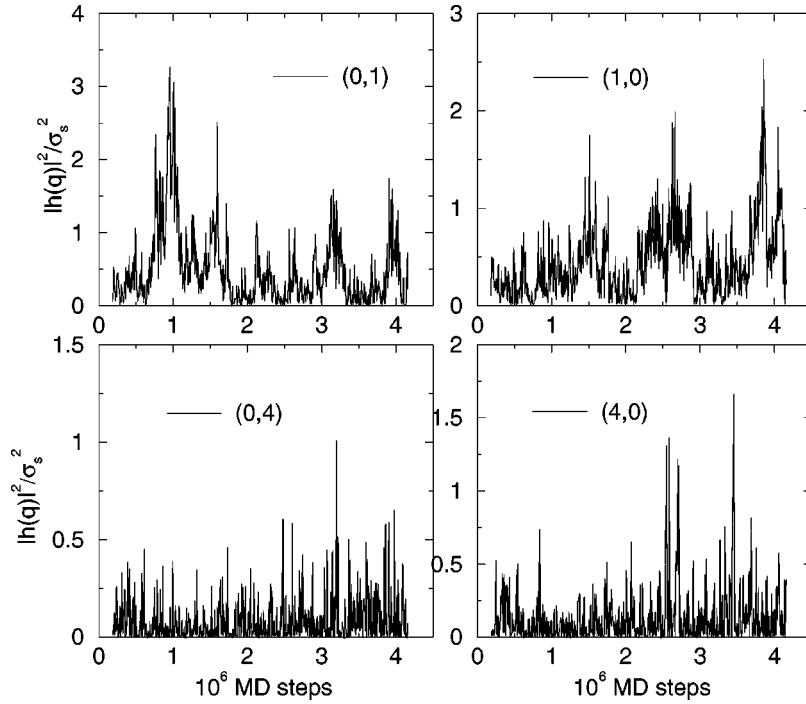
FIG. 3. Fourier modes $|h(\mathbf{q})|^2$ for $n=(0,1)$, $(1,0)$, $(0,4)$, and $(4,0)$ vs time in units of MD steps.

where

$$s^2 = \langle h^2(x,y)\rangle = \frac{1}{4\pi^2}\int d\mathbf{q}\langle|h(\mathbf{q})|^2\rangle = \frac{1}{2\pi\gamma}\ln\left(\frac{q_{max}}{q_{min}}\right). \tag{10}$$

The lower and upper cutoffs $q_{max}=2\pi/B$ and $q_{min}=2\pi/L$ come into play, because the integral $\int d\mathbf{q}\langle|h(\mathbf{q})|^2\rangle \sim \int dq/q$ diverges as $q\to 0$ and $q\to\infty$. The actual local height distribution $P(h)$ obtained from our simulations is plotted for several block sizes in Fig. 5. It can be fitted nicely by a Gaussian distribution (9).

Next, we study the width ω of the average order-parameter profile as a function of the block size. According

to the capillary-wave theory, the capillary-wave fluctuations broaden it for large blocks B according to

$$\omega^2 = \omega_0^2 + \frac{\pi}{2}s^2 = \omega_0^2 + \frac{k_B T}{4\gamma}\ln\left(\frac{\hat{q}_{max}}{\hat{q}_{min}}\right). \tag{11}$$

Here the cutoff wave vectors are given by $\hat{q}_{min}=2\pi/B$ and $\hat{q}_{max}=2\pi/a_0$, where a_0 is a microscopic length which need not be specified here.

The broadening effect is demonstrated for different block sizes B in Fig. 6. The interfacial width can be estimated by fitting order-parameter profiles such as those shown in Fig. 6 to *tanh* profiles,
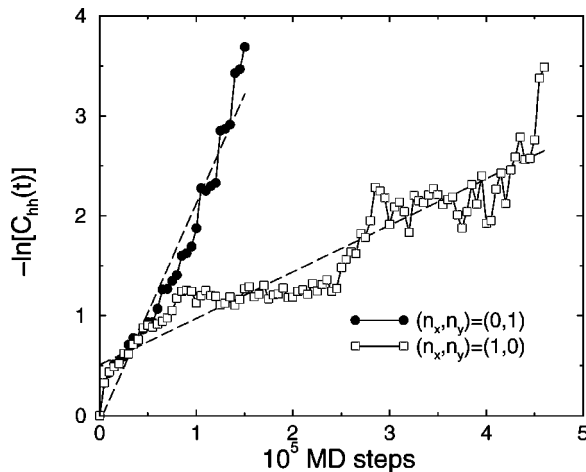

FIG. 4. Autocorrelation function C_{hh} vs MD steps for the two slowest modes $\mathbf{n}=(1,0)$ (normal to the director) and of $\mathbf{n}=(0,1)$ (parallel to the director).
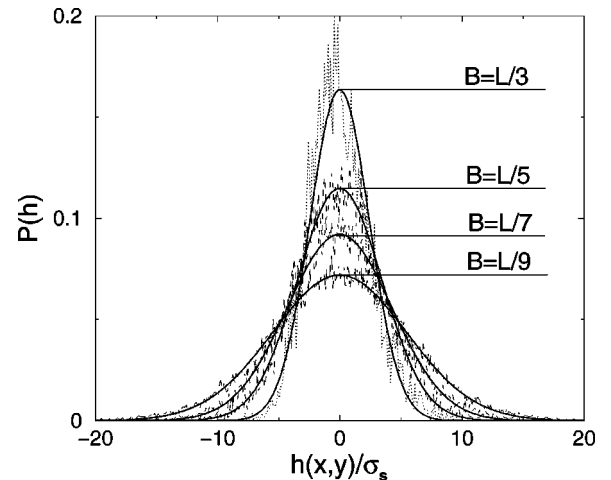

FIG. 5. Distribution of local interface positions for block sizes $B=L/3$, $L/5$, $L/7$, and $L/9$. The solid lines are Gaussian fits [Eq. (9)].
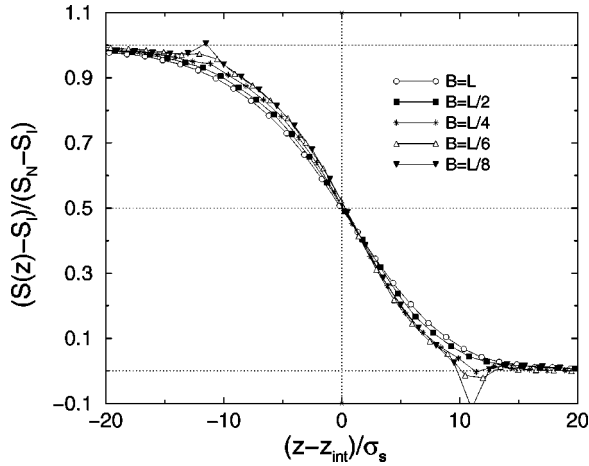
FIG. 6. Order-parameter profiles for block sizes $B=L$, $L/2$, $L/4$, $L/6$, and $L/8$. S_N and S_I are the average values of the order parameter in the nematic and isotropic phase, respectively.

$$S(z) = \frac{1}{2}(S_N + S_I) + \frac{1}{2}(S_N - S_I)\tanh\left(\frac{z-z_{int}}{\omega}\right), \quad (12)$$

where the parameters S_N and S_I are the values of the order parameter in the bulk nematic and isotopic phases. (Note that S_I is nonzero due to the finite number of particles in a bin.) Figure 7 plots the squared interfacial width ω^2 as a function of block size B. One clearly observes the logarithmic increase of ω^2 with block size B predicted by Eq. (11). From the slope of the line one can estimate the interfacial tension, $\gamma = 0.016 \pm 0.002 k_B T/\sigma_s^2$.

For comparison, we have also determined the interfacial tension from the anisotropy of the pressure tensor, making use of the relation [16,11]

$$\gamma = \int_{-\infty}^{\infty} dz[P_N(z) - P_T(z)], \quad (13)$$

where P_N and P_T are the normal and transverse pressure tensor components. Here we consider particles with pair in-
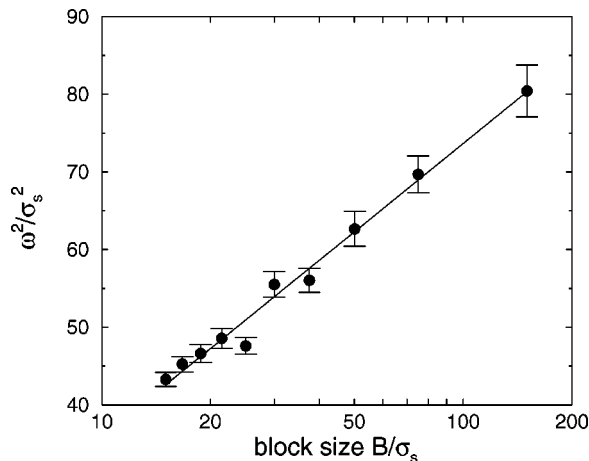

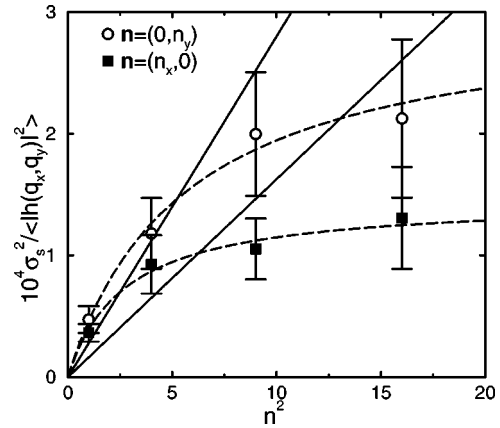FIG. 7. Squared interfacial width ω^2 vs block size B. The solid line is a fit to Eq. (11).

FIG. 8. Inverse of the mean-squared Fourier components of the interface position $1/\langle|h(\mathbf{q})|^2\rangle$ vs q^2 for parallel (circle) and normal (square) to the director. Dashed lines are guides to eye. Lines corresponds to the prediction of simple capillary-wave theory of Eq. (2) with $\gamma = 0.016\sigma_s^2/k_B T$ (solid line), and $\gamma = 0.0093\sigma_s^2/k_B T$ (dashed line).

teractions V_{ij}, Eq. (3) and systems with two interfaces in the (xy) plane. Neglecting finite-size effects and interactions between the interfaces, Eq. (13) thus reads

$$\gamma = \frac{1}{4L^2} \sum_{i<j} \left\langle r_{ij}^x \frac{\partial V_{ij}}{\partial r_{ij}^x} + r_{ij}^y \frac{\partial V_{ij}}{\partial r_{ij}^y} - 2 r_{ij}^z \frac{\partial V_{ij}}{\partial r_{ij}^z} \right\rangle. \quad (14)$$

The simulation data yield $\gamma = 0.0093 \pm 0.003\sigma_s^2/k_B T$. This value agrees with earlier results obtained in smaller systems [17]. It is of the same order, but smaller than the value estimated from the interfacial broadening. The quantitative difference possibly stems from attractive interactions between the two interfaces of the nematic slab. More simulations, in which the thickness of the slab is varied systematically, would be needed to elucidate this point.

Finally, we turn to the analysis of the capillary-wave spectrum $\langle|h(\mathbf{q})|^2\rangle$, which is predicted to be inversely proportional to q^2 according to Eq. (2). We study separately the $\mathbf{q}$ direction parallel $[\mathbf{q} \propto (0,1)]$ and perpendicular $[\mathbf{q} \propto (1,0)]$ to the director. The inverse of $\langle|h(\mathbf{q})|^2\rangle$ in these two directions is shown in Fig. 8 as a function of the squared wave vectors. In the long-wavelength limit $\mathbf{q} \to 0$, the spectrum appears to be isotropic, and $1/\langle|h(\mathbf{q})|^2\rangle$ approaches zero in agreement with the capillary-wave theory. The initial slope is consistent with Eq. (2) if one uses $\gamma = 0.016 k_B T/\sigma_s^2$, and still roughly compatible if one uses $\gamma = 0.0093 k_B T/\sigma_s^2$. As $\mathbf{q}$ increases, the capillary-wave spectrum becomes anisotropic. As one might expect intuitively, the amplitudes $\langle|h(\mathbf{q})|^2\rangle$ are larger for capillary waves in the direction perpendicular to the director.

Deviations of capillary-wave spectra from the straight line predicted by the simple capillary-wave theory (2) are often discussed in terms of higher-order terms in the capillary-wave Hamiltonian (1), i.e., terms proportional to squares of higher-order derivatives of $h(x,y)$. For example, including the next-to-leading term leads to a prediction of the form $1/\langle|h(\mathbf{q})|^2\rangle \propto \gamma q^2 + \delta q^4$, where γ is the interfacial tension

and δ is a bending rigidity. One might intuitively expect that the *N-I* interface has bending stiffness, based on the argument that the elastic interactions should penalize interfacial bending.

However, Fig. 8 indicates that the sign of the ''bending energy'' is *negative*. The naive argument sketched above is thus clearly wrong. On the contrary, our unexpected result suggests that the elastic interactions influence the capillary waves on the largest length scale: The interface is rougher on short-length scales than one would expect from the long-wavelength fluctuations. This observation is consistent with our speculations in the introduction, that the elastic interactions may be responsible for the suppression of capillary-wave fluctuations of the *N-I* interface in the Onsager limit of infinitely elongated particles.

We note that this is not the first observation of a negative bending rigidity at a fluid-fluid interface. A similar phenomenon has been predicted theoretically for liquid-vapor interfaces [18,20] and verified experimentally by Fradin *et al.* [21]. The negative bending rigidity is attributed in their case to long-range van der Waals interactions [19]. Indications of

a negative bending rigidity at a liquid-liquid interface have also been found in molecular-dynamics simulations of simple liquids by Stecki and Toxvaerd [22,23].

To summarize, we have studied the *N-I* interface by large scale molecular-dynamics simulation of a system of repulsive ellipsoidal molecules. We find that the standard capillary-wave theory explains most of our results very well. Discrepancies are encountered when looking at the amplitudes of capillary-wave modes at large wave vectors, i.e., on small length scales. We find that they are smaller than expected and anisotropic.

[1] P. G. de Gennes and J. Prost, *The Physics of Liquid Crystals*, 2nd ed. (Clarendon Press, Oxford, 1993).

[2] B. Jerome, Rep. Prog. Phys. **54**, 391 (1991).

[3] L. Onsager, Ann. (N.Y.) Acad. Sci. **51**, 627 (1949).

[4] Z. Y. Chen and J. Noolandi, Phys. Rev. A **45**, 2389 (1992).

[5] D. L. Koch and O. G. Harlen, Macromolecules **32**, 219 (1999).

[6] M. P. Allen, J. Chem. Phys. **112**, 5447 (2000).

[7] F. P. Buff, R. A. Lovett, F. H. Stillinger, Phys. Rev. Lett. **15**, 621 (1965).

[8] J. S. Rowlinson and B. Widom, *Molecular Theory of Capillarity* (Clarendon, Oxford, 1982).

[9] Y. Mao, M. E. Cates, and H. N. W. Lekkerkerker, J. Chem. Phys. **106**, 3721 (1997).

[10] M. A. Bates and C. Zannoni, Chem. Phys. Lett. **280**, 40 (1997).

[11] A. J. McDonald, M. P. Allen, and F. Schmid, Phys. Rev. E **63**, 010701 (2000).

[12] J. G. Gay and B. J. Berne, J. Chem. Phys. **74**, 3316 (1981).

[13] B. J. Berne and P. Pechukas, J. Chem. Phys. **56**, 4213 (1975).

[14] A. Werner, F. Schmid, M. Müller, and K. Binder, Phys. Rev. E **59**, 728 (1999).

[15] J. D. Weeks, J. Chem. Phys. **67**, 3106 (1977); D. Bedeaux and J. D. Weeks, *ibid.* **82**, 972 (1985).

[16] P. Schofield and J. R. Henderson, Proc. R. Soc. London, Ser. A **379**, 231 (1982).

[17] The simulations of Ref. [11] yielded the interfacial tension $\gamma = 0.011\sigma_s^2/k_BT$. However, the systems studied there were so small that the actual value of γ is not very reliable.

[18] E. M. Blokhuis and D. Bedeaux, Mol. Phys. **80**, 705 (1993).

[19] For a more general discussion of bending rigidities in isotropic fluids with arbitrary pair interactions see also N. Napiorkowsky and S. Dietrich, Phys. Rev. E **47**, 1836 (1993); Z. Phys. B: Condens. Matter **97**, 511 (1995).

[20] K. R. Mecke and S. Dietrich, Phys. Rev. E **59**, 6766 (1999).

[21] C. Fradin, D. Luzet, D. Smilgies, A. Braslau, M. Alba, N. Boudet, K. Mecke, and J. Daillant, Nature (London) **403**, 871 (2000).

[22] J. Stecki and S. Toxvaerd, J. Chem. Phys. **103**, 9763 (1995).

[23] E. M. Blokhuis and D. Bedeaux, Mol. Phys. **96**, 397 (1999).